

Special purpose quantum graphs for guaranteed and fast search times

Quancheng Liu, David A. Kessler, and Eli Barkai

Department of Physics, Institute of Nanotechnology and Advanced Materials, Bar-Ilan University, Ramat-Gan 52900, Israel

(Dated: February 9, 2022)

We design monitored quantum walks with the aim of optimizing state transfer and target search. We show how to construct walks with the property that all the eigenvalues of the non-Hermitian survival operator, describing the mixed effect of unitary dynamics and the back-action of measurement, coalesce to zero, corresponding to an exceptional point whose degree is the size of the Hilbert space. Generally, this search is guaranteed to succeed in a bounded time for any initial condition. It also performs better than the classical random walk search or quantum search on typical graphs. For example, a crawler can be designed such that, starting on a node of the graph, the walker is detected on any of the nodes with probability one at predetermined times. It also allows perfect quantum state transfer from one node of the system to any other, with or without monitoring. Interestingly, this crawler is described as a massless Dirac quasi-particle.

The goal of quantum state transfer is to transform a state $|\psi_0\rangle$ to a predetermined target state $|\psi_d\rangle$, in particular in relatively large systems [1, 2]. For example, the initial state could be an entry node of a chain and the final state the exit node [3]. This basic idea finds applications in quantum search algorithms [4], light-harvesting systems [5, 6], quantum information [7, 8], and the problem of escape from a maze [9]. With unitary evolution, perfect quantum transfer $|\langle\psi_d|\psi(t)\rangle|^2 = 1$; with $|\psi(t=0)\rangle = |\psi_0\rangle$ was found for some particular time t in large specially constructed spin systems [3], while typical systems fall far from this limit. A question left open is can we design a system that perfectly transfers $|\psi\rangle$ among all the N states of the system, instead of between a specific pair. Namely we search for a system such that at specified times t_i and for specified states $|x_i\rangle$ (nodes of the system, say), $|\langle x_i|\psi(t_i)\rangle|^2 = 1$. In the context of quantum walks [10, 11] this gives an option of transferring a state localized on one spatial node to *any* other node in the system, without modifying the underlying Hamiltonian. This will be shown to be possible with a specifically designed unitary quantum walk.

However, not in all cases do we have information on the initial state. In this situation, to find the walker in the target state we use the following strategy [12–18]: every τ units of time we check with a local measurement (see below) whether the walker is on a specific node $|\psi_d\rangle$. Extending the concept of perfect state transfer, we search for a method where the target state is detected with probability one before some final fixed time t and with a finite number of measurements. We call such a process a guaranteed search, as the detection/transfer within a fixed time is assured. In other words, while usual quantum transfer assumes complete knowledge of the initial condition, and the goal is to maximize the success probability of the unitary evolution $|\langle\psi_d|\psi(t)\rangle|^2$ at some fixed time, if we have no knowledge about the initial state, we aim to detect the final state $|\psi_d\rangle$ within some fixed and finite time.

As shown below, the two mentioned problems are re-

lated. We propose special purpose quantum graphs, designing tight-binding Hamiltonians that have remarkable search capabilities both for the monitored and non-monitored cases, and either with or without control of the initial state. One of the features of efficient quantum search we find here is that it is intimately related to the study of exceptional points. The latter are degenerate eigenvalues of the non-Hermitian operators that are studied, for example, in optics and laser physics [19–22], topological phases [23–26], and are fundamentally related to parity-time symmetry breaking [27–29]. Here, we design a graph and search protocol with an exceptional point of unusually high degeneracy, namely the size of Hilbert space, which in principle can be made as large as we wish. We highlight the idea that exceptional search is found when all the eigenvalues of the survival operator, defined below, coalesce to zero creating a large degeneracy. Towards the end of the paper we show how the search problem and the corresponding degeneracy of the exceptional points are related to an effective massless Dirac particle, though all along we use Schrödinger dynamics.

Model.—The first-passage time [30, 31] to a given target state $|\psi_d\rangle$ is not a physical observable in the quantum world [32], given the absence of a well-defined trajectory. Instead, the concept of a monitored quantum walk is used [12–18, 33]. In the stroboscopic protocol, which as we show later is an efficient tool, we project the state $|\psi_d\rangle$ at times $\tau, 2\tau, \dots$ and at each measurement ask if the system is found at its target. This yields a string of no, no, \dots , and in the n -th measurement a yes. Once we record a yes, the system is at state $|\psi_d\rangle$ and in that sense we have a monitored state transfer. The time $n\tau$ is the first detection time of the state $|\psi_d\rangle$, which is clearly a random variable whose statistical properties ultimately depend on the initial state of the system $|\psi_{in}\rangle$, the unitary evolution between measurements, and the choice of τ . We will show later how this monitored protocol is related to unitary state transfer without measurements.

Let F_n be the probability of detecting the system in

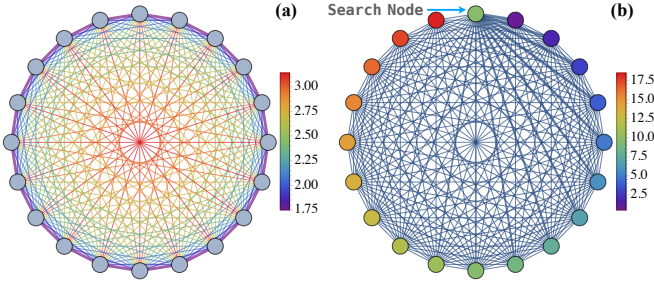


FIG. 1. Schematic presentation of the crawl graph (a) and funnel model (b). Here $N = 20$. The thickness of the connecting line represents the strength of the matrix element connecting two nodes [(a) and (b)]. The colors represent the phases of the hopping rates (a). In (b) we utilize colors to represent the magnitude of the on-site energies, whose matrix elements are real (see details in SM). The crawl graph exhibits perfect quantum state transfer between any pair of nodes in the system, with or without monitoring. The search on both graphs is guaranteed to succeed within a bounded time, for any initial condition.

state $|\psi_d\rangle$ for the first time at $n\tau$. This basic probability is given in terms of the amplitude ϕ_n of first detection, namely $F_n = |\phi_n|^2$ with [15, 16, 18, 33–35]

$$\phi_n = \langle \psi_d | U(\tau) \mathcal{S}^{n-1}(\tau) | \psi_{in} \rangle, \quad (1)$$

where the survival operator is $\mathcal{S}(\tau) = (1 - |\psi_d\rangle \langle \psi_d|) U(\tau)$. Here the back-action of the previous $n - 1$ repeated measurements is to project out the amplitude of the detected state. In Eq. (1) we use the basic postulates of quantum theory with the projection $1 - |\psi_d\rangle \langle \psi_d|$. The probability of eventual detection is $P_{\text{det}} = \sum_{n=1}^{\infty} F_n$, and if $P_{\text{det}} = 1$ the mean time for first detection is $\langle t \rangle = \tau \sum_{n=1}^{\infty} n F_n$.

As usual with these types of problems, the eigenvalues of $\mathcal{S}(\tau)$ are essential for the characterization of the process. The eigenvalues of $\mathcal{S}(\tau)$, denoted ξ , are all in or on the unit circle $|\xi| \leq 1$, and the eigenvalues $|\xi| = 1$ correspond to dark states [13, 34, 36]. Our goal is to find $U(\tau)$ and the corresponding H so that all the eigenvalues of $\mathcal{S}(\tau)$ are equal to zero. Intuitively, if all the eigenvalues are very small, the decay of F_n is expected to be fast. It is also clear that if we find such an H , the eigenvalues ξ coalesce to the value $\xi = 0$ [37], meaning that we are engineering a method that yields a survival operator whose spectrum N -fold degenerate, N being the size of the Hilbert space.

The eigenvalues ξ are given by

$$\det|\xi - \mathcal{S}(\tau)| = \xi \det|\xi - U(\tau)| \langle \psi_d | \frac{1}{\xi - U(\tau)} | \psi_d \rangle = 0 \quad (2)$$

where we have used the matrix determinant lemma, see supplementary material [SM]. Clearly the system always has at least one solution $\xi = 0$. Let $H|E_k\rangle = E_k|E_k\rangle$ where $k = 0, \dots, N - 1$ and as usual we may expand

$|\psi_d\rangle = \sum_{k=0}^{N-1} \langle E_k | \psi_d \rangle |E_k\rangle$, and then

$$\langle \psi_d | \frac{1}{\xi - U(\tau)} | \psi_d \rangle = \sum_{k=0}^{N-1} \frac{p_k}{\xi - \exp(-iE_k\tau)} \quad (3)$$

while $\det|\xi - U(\tau)| = \prod_{k=0}^{N-1} [\xi - \exp(-iE_k\tau)]$. Here $p_k = |\langle E_k | \psi_d \rangle|^2$ is the square of the overlap between the energy state $|E_k\rangle$ and the detected state. Our first requirement is that the system is such that $p_k \neq 0$ for all the energy states $|E_k\rangle$, and that there is no degeneracy i.e., $\exp(-iE_k\tau) \neq \exp(-iE_m\tau)$ for any choice of $m \neq k$. Physically this demand means that we exclude dark states so $|\xi| < 1$ and hence the eigenvalues satisfy $\det|\xi - U(\tau)| \neq 0$. Using Eqs. (2,3) it is not difficult to show that the eigenvalue problem reduces to finding the solution of

$$\xi \sum_{k=0}^{N-1} \frac{p_k}{\xi - \exp(-iE_k\tau)} = 0. \quad (4)$$

We now engineer the system in such a way that the only degenerate solution is $\xi = 0$. To reach this goal, we found the following requirements

$$p_k = \frac{1}{N} \quad \text{and} \quad E_k\tau = \frac{2\pi k}{N}. \quad (5)$$

We see that the energy levels must be equally spaced, which intuitively is expected as this causes the periodicities in the dynamics to resonate at specific times, enhancing constructive interference. More specifically, we will soon choose $E_k = \gamma k$ where γ has units of energy, and then $\tau = 2\pi/\Delta E$ where $\Delta E = E_{\text{max}} - E_{\text{min}}$ is the energy gap between the ground and largest energy in the spectrum. We also see that the overlap p_k must be k -independent. To verify these requirements, insert Eq. (5) in Eq. (4) and then with summation formulas (see SM) we have

$$\frac{\xi}{N} \sum_{k=0}^{N-1} \frac{1}{\xi - \exp(-i2\pi k/N)} = -\frac{\xi^N}{1 - \xi^N} = 0 \quad (6)$$

and the only possible solution is $\xi = 0$. We see that for a quantum system satisfying Eq. (5), the survival operator has a N -fold degenerate eigenvalues at $\xi = 0$, as we aimed for. Further all the right and left eigenvectors also coalesce. Before constructing the graph that yields this result we study the general consequences for search.

We denote H_s , U_s and \mathcal{S}_s the Hamiltonian, unitary and survival operator for a system that satisfies the efficient search conditions Eq. (5) and in this notation we omit the dependence on τ . We define the states $|Q_k\rangle = (U_s)^k |\psi_d\rangle$ with $k = 0, \dots, N - 1$. The operators U_s and \mathcal{S}_s acting on these states give

$$\begin{aligned} U_s |Q_{N-1}\rangle &= |\psi_d\rangle, & U_s |Q_k\rangle &= |Q_{k+1}\rangle \text{ if } k \neq N - 1, \\ \mathcal{S}_s |Q_{N-1}\rangle &= 0, & \mathcal{S}_s |Q_k\rangle &= |Q_{k+1}\rangle \text{ if } k \neq N - 1. \end{aligned} \quad (7)$$

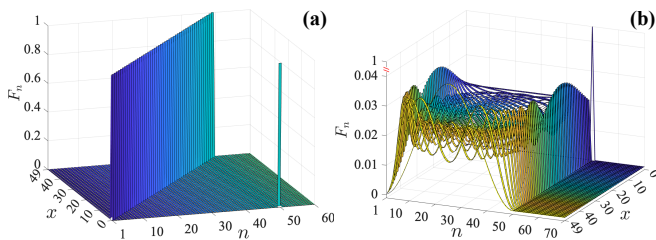


FIG. 2. Detection probability F_n versus n for the crawl (a) and funnel (b) model. Here the graph has $N = 50$ nodes and we present results with initial states localized on one of the nodes $|\psi_{\text{in}}\rangle = |x\rangle$, $x = 0, 1, \dots$ and $|\psi_{\text{d}}\rangle = |0\rangle$. For the crawl search we find a deterministic outcome of the process, where $F_n = 1$ when $n = x$ (for $x = 0$, $F_{50} = 1$). For the funnel model (b) notice the sharp cutoff of F_n for $n > N = 50$. For any initial condition, the detection of the state is guaranteed with probability one, within at most N measurements, which we call guaranteed search. In (b) notice the peak of height one for $n = 50$, when the initial condition is the same as the detected state. The upper bound for the search time is $t_{\text{max}} = \tau N = 2\pi$.

We see that both \mathcal{S}_s and U_s are shift operators, the difference is the action on the boundary term $|Q_{N-1}\rangle$. We can also show that the states $|Q_k\rangle$ are orthonormal $\langle Q_l | Q_m \rangle = \delta_{lm}$ (see SM) and they form a complete set spanning any initial condition in the Hilbert space. From here we reach the following conclusions. First, consider an initial condition which is a $|Q_k\rangle$ state, then following Eq. (1) we consider the operation $(\mathcal{S}_s)^n |Q_k\rangle$ and using Eq. (7)

$$\phi_n = \begin{cases} 1 & \text{if } n = N - k, \\ 0 & \text{otherwise.} \end{cases} \quad (8)$$

This means that we detect the target with probability one at time $(N - k)\tau$, hence the detection process is deterministic as the fluctuations of the detection time vanish. For a more general initial condition, exploiting the fact that the states $|Q_k\rangle$ form a complete set and the linearity of Eq. (1) with respect to the initial condition, the probability of first detection $F_n = |\phi_n|^2$ is

$$F_n = \begin{cases} |\langle Q_{N-n} | \psi_{\text{in}} \rangle|^2 & \text{for } n = 1, \dots, N, \\ 0 & \text{otherwise.} \end{cases} \quad (9)$$

This implies a guaranteed search, since even in the absence of knowledge about the initial condition, the search will find the target with at most N operations. From here it also follows that we have an upper bound on the mean search time $\langle t \rangle \leq \tau N = 2\pi k / E_k = 2\pi / \gamma$. This upper bound is N independent, so that the maximum search time does not scale with the system size. The upper limit is found when the initial condition is the target state $|\psi_{\text{in}}\rangle = |\psi_{\text{d}}\rangle$.

What are the tight-binding Hamiltonians of size $N \times N$, that yields the guaranteed search? The condition Eq. (5) admits many types of solutions, and here we present

two that have certain advantages. First, we present an approach where the nodes of the graph are the states $|Q_k\rangle$. This is clearly useful since this means that we can start the process with the wave packet on one node of the graph and find the walker with probability one after a fixed time at any other node, which we call deterministic search as the fluctuations vanish. We use $H = \sum_k E_k |E_k\rangle \langle E_k|$ and for the equal distance energies we set $E_0 = 0, E_1 = \gamma, \dots, E_{N-1} = (N-1)\gamma$ and Eq. (5) gives $\tau = 2\pi / N\gamma$ [38]. In this system the states $|x\rangle$ with $x = 0, 1, \dots, N-1$ are the nodes of the graph, see Fig. 1. Furthermore, this model can exhibit perfect quantum state transfer between all the nodes in the system. To perform this trick let

$$|E_k\rangle = \left\{ 1, e^{i\theta_k}, e^{i2\theta_k}, \dots, e^{i(N-1)\theta_k} \right\}^T / \sqrt{N} \quad (10)$$

where $\theta_k = 2\pi k / N$. This eigenstate is a discrete Fourier wave, which is related to the “relativistic” linear dispersion in Eq. (5), and Dirac physics as discussed below. Clearly Eq. (10) gives $p_k = 1/N$ and hence

$$\gamma \begin{bmatrix} 0 & \frac{1}{1-e^{i\theta_1}} & \frac{1}{1-e^{i\theta_2}} & \dots & \frac{1}{1-e^{i\theta_{N-1}}} \\ \frac{1}{1-e^{-i\theta_1}} & 0 & \frac{1}{1-e^{-i\theta_1}} & \dots & \frac{1}{1-e^{-i\theta_{N-2}}} \\ \frac{1}{1-e^{-i\theta_2}} & \frac{1}{1-e^{-i\theta_1}} & 0 & \dots & \frac{1}{1-e^{-i\theta_{N-3}}} \\ \vdots & \vdots & \vdots & \ddots & \vdots \\ \frac{1}{1-e^{-i\theta_{N-1}}} & \frac{1}{1-e^{-i\theta_{N-2}}} & \frac{1}{1-e^{-i\theta_{N-3}}} & \dots & 0 \end{bmatrix} \quad (11)$$

which we call the Crawl Hamiltonian, see schematics in Fig. 1(a). This system, as discussed below, breaks time-reversal symmetry. In Fig. 2(a) we plot F_n for a system with $N = 50$ and where the target state is $|\psi_{\text{d}}\rangle = |0\rangle$. We choose local initial conditions such that $|\psi_{\text{in}}\rangle = |x\rangle$, hence we are considering a transition from x to 0 and in the plot we choose $x = 0, 1, \dots, 49$. We see that F_n is sharply peaked and is equal to unity when $n = x$. This type of deterministic search is not found for classical random walks, and relies on the fact that the quantum wave packet can, at specific times of the evolution, be localized on a single node, while at prior measurement times the wave packet is vanishing on the node. We will soon show that the *non-monitored* wave packet exhibits the desired unity success probability on all the nodes of the system one after the other.

We now consider an alternative approach, which we term the funnel model, that uses on-site energies to direct the search to a specific node denoted $|\psi_{\text{d}}\rangle = |0\rangle$. We still have condition Eq. (5) to fulfill and we start with $|E_0\rangle = \{1/\sqrt{N}, -\sqrt{(N-1)/N}, 0, \dots\}^T$. The next energy state is constructed such that it is normalized and orthogonal to $|E_0\rangle$ and has an overlap $1/N$ with the search target, $|E_1\rangle = \{1/\sqrt{N}, 1/\sqrt{N(N-1)}, -\sqrt{(N-2)/(N-1)}, 0, \dots\}^T$. The process of constructing these states is continued,

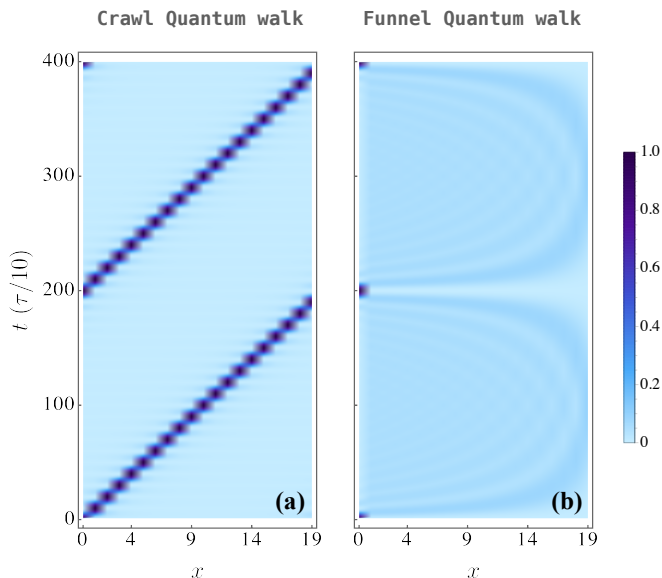


FIG. 3. The time evolution of the wave packet on the crawl (a) and funnel (b) graphs for non-monitored quantum walks. The color code gives the probability of finding the walker on a node. For the crawl graph, the wave function is fully localized one node after the other at times $\tau, 2\tau, \dots$, a feature which is vital for state transfer to any node in the system. In addition, the uni-directional movement of the packet can be inverted by changing H_{Crawl} to its complex H_{Crawl}^* , which is a feature of time-reversal symmetry. Both quantum walks exhibit revival, namely the wave function returns to its initial state, at time $N\tau$.

and then exploiting the demand that energy levels are equidistant we find H , which is provided explicitly in SM and presented schematically in Fig. 1(b). Here the Hamiltonian does not break time-reversal symmetry. In Fig. 2(b) we present the detection probabilities for localized initial conditions. Fig. 2 illustrates a sharp cutoff, namely $F_n = 0$ for any $n > N$ and thus the search is guaranteed to succeed in a finite time, as predicted in Eq. (9). This feature is completely absent in classical random walks or quantum walks on non-specialized graphs. If the initial state is the same as the detected one, $F_{50} = 1$ otherwise it is zero, a feature which is universal for all search graphs satisfying Eq. (5).

We now move from repeated measurements and consider state transfer with unitary dynamics. First consider H_{Crawl} and assume we start on a node and want to transfer the system on another node without repeated measurements. From the fact that both \mathcal{S}_s and U_s are shift operators, this is precisely the case. Namely, if we start on a node $|\psi_0\rangle = |x_0\rangle$ and focus on the target node $|\psi_a\rangle = |x_f\rangle$ the (non-monitored) success probability is

$$|\langle \psi(t) | \psi_a \rangle|^2 = 1 \quad (12)$$

at times $t = (x_f - x_0)\tau$. Hence, as shown in Fig. 3(a), the wave packet is completely localized one node after

the other, advancing like the hands of a perfect clock covering the node space efficiently. The amplitude vanishes elsewhere in the system. Hence we may transfer the wave packet from one node to another, i.e. detect the walker with probability one with one perfectly timed measurement. By comparison, in the funnel model we see the revival of the state function in the initial state, an effect that takes place for any model satisfying Eq. (5), even when the system size is large. However, the crawling effect on the nodes of the system is absent (see Fig. 3(b)).

The efficient state transfer we found here is reminiscent of the physics of a massless Dirac particle in dimension one. First the energy is linear in k . Second in the crawl model the energy states are discrete free waves, and finally due to time-reversal breaking, the wave packet can travel either clockwise or anti-clockwise (on the graph of Fig. 1(a)), somewhat similar to the particle and anti-particle. But why is Dirac physics related to perfect quantum state transfer?

We started this work with the demand that the eigenvalues of \mathcal{S} , are real and all coalesce to zero, in order to speed up search and create a tool for efficient state transfer. As illustrated in Fig. 3(a), the fact that the wave packet is not widening is crucial for the validity of Eq. (12). Namely, if the packet is spreading we cannot reach a perfect detection with probability one. Physically, for a Dirac massless particle, the wave packet does not widen while propagating, and this in turn allows precise state transfer. Consider the wave equation in continuous space, $\partial_x \psi(x, t) = \partial_t \psi(x, t)$, the solution is $\psi(x, t) = \int dk g(k) \exp(i(kx - w_k t))$ and $g(k)$ is the initial packet in momentum space. For spatially localized initial condition and using $w = k$ we get a delta traveling wave, in close analogy with what we find in discrete space. Of course the underlying dynamics in our case is controlled by the Schrödinger equation, but the Hamiltonian under study yields an effective motion in which space and time are treated on the same footing. Finally, the Dirac wave function in dimension one has two components. Similarly, we have a particle traveling clockwise and anti-clockwise. We can switch between these modes by replacing the Hermitian H_{Crawl} with its complex conjugate.

Our proposal is based on current technologies that allow clever engineering of Hamiltonians with waveguide arrays [9, 39–43], trapped ions [44, 45], Josephson junctions [46–48], cold atoms [49], etc. For example, in photonic systems, artificial gauge fields have been experimentally induced through a harmonic modulation of the refractive index [50, 51], introducing complex-valued controllable couplings between waveguides [39–41, 43]. These advances allow us to consider the option of constructing a device with non-trivial matrix elements $H_{i,j}$ and thus design in the laboratory special types of graphs to speed up the search and generate perfect quantum

state transfer.

To summarize, we have designed a survival operator $S(\tau)$, with an exceptional point whose degeneracy is the size of the Hilbert space. The resulting special purpose family of Hamiltonians allows for guaranteed search. For specialized states $|Q_i\rangle$ the monitored search process is deterministic as the fluctuations in the detection attempt vanish. The main condition Eq. (5) still allows for further freedom in the design of the search process. For the crawl model the search is effectively uni-directional in a system that conserves energy. The (non-monitored) success probability is unity, and the state transfer can be made efficient from any spatial starting point to any other node of the graph. The Hamiltonian is independent of the choice of the target state, and in that sense the system exhibits what we call universal search. Further the search is globally optimal with respect to any other search algorithm, in the sense that the success probability is unity even for large systems and for all the nodes.

Acknowledgments: E.B. thanks Shimon Yankelevich, Moshe Goldstein, and Lev Khaikovich for comments and suggestions. The support of Israel Science Foundation's grant 1614/21 is acknowledged.

-
- [1] J. I. Cirac, P. Zoller, H. J. Kimble, and H. Mabuchi, "Quantum state transfer and entanglement distribution among distant nodes in a quantum network," *Phys. Rev. Lett.* **78**, 3221 (1997).
- [2] A. Reiserer and G. Rempe, "Cavity-based quantum networks with single atoms and optical photons," *Rev. Mod. Phys.* **87**, 1379 (2015).
- [3] M. Christandl, N. Datta, A. Ekert, and A. J. Landahl, "Perfect state transfer in quantum spin networks," *Phys. Rev. Lett.* **92**, 187902 (2004).
- [4] A. M. Childs and J. Goldstone, "Spatial search by quantum walk," *Phys. Rev. A* **70**, 022314 (2004).
- [5] J. Cao *et al.*, "Quantum biology revisited," *Sci. Adv.* **6**, eaaz4888 (2020).
- [6] N. Dudhe, P. K. Sahoo, and C. Benjamin, "Testing quantum speedups in exciton transport through a photosynthetic complex using quantum stochastic walks," (2021), [arXiv:2004.02938](https://arxiv.org/abs/2004.02938).
- [7] H. J. Kimble, "The quantum internet," *Nature* **453**, 1023 (2008).
- [8] T. E. Northup and R. Blatt, "Quantum information transfer using photons," *Nat. Photonics* **8**, 356 (2014).
- [9] F. Caruso, A. Crespi, A. G. Ciriolo, F. Sciarrino, and R. Osellame, "Fast escape of a quantum walker from an integrated photonic maze," *Nat. Commun.* **7**, 11682 (2016).
- [10] O. Mülken and A. Blumen, "Continuous-time quantum walks: Models for coherent transport on complex networks," *Phys. Rep.* **502**, 37 (2011).
- [11] A. M. Childs, "Universal computation by quantum walk," *Phys. Rev. Lett.* **102**, 180501 (2009).
- [12] H. Krovi and T. A. Brun, "Quantum walks with infinite hitting times," *Phys. Rev. A* **74**, 042334 (2006).
- [13] H. Krovi and T. A. Brun, "Hitting time for quantum walks on the hypercube," *Phys. Rev. A* **73**, 032341 (2006).
- [14] H. Krovi and T. A. Brun, "Quantum walks with infinite hitting times," *Phys. Rev. A* **74**, 042334 (2006).
- [15] F. A. Grünbaum, L. Velázquez, A. H. Werner, and R. F. Werner, "Recurrence for discrete time unitary evolutions," *Commun. Math. Phys.* **320**, 543 (2013).
- [16] S. Dhar, S. Dasgupta, A. Dhar, and D. Sen, "Detection of a quantum particle on a lattice under repeated projective measurements," *Phys. Rev. A* **91**, 062115 (2015).
- [17] S. Lahiri and A. Dhar, "Return to the origin problem for a particle on a one-dimensional lattice with quasi-zeno dynamics," *Phys. Rev. A* **99**, 012101 (2019).
- [18] F. Thiel, E. Barkai, and D. A. Kessler, "First detected arrival of a quantum walker on an infinite line," *Phys. Rev. Lett.* **120**, 040502 (2018).
- [19] M. A. Miri and A. Alù, "Exceptional points in optics and photonics," *Science* **363**, eaar7709 (2019).
- [20] M. Liertzer, L. Ge, A. Cerjan, A. D. Stone, H. E. Türeci, and S. Rotter, "Pump-induced exceptional points in lasers," *Phys. Rev. Lett.* **108**, 173901 (2012).
- [21] J. Doppler *et al.*, "Dynamically encircling an exceptional point for asymmetric mode switching," *Nature* **537**, 76 (2016).
- [22] H. Xu, D. Mason, L. Jiang, and J. G. E. Harris, "Topological energy transfer in an optomechanical system with exceptional points," *Nature* **537**, 80 (2016).
- [23] T. E. Lee, "Anomalous edge state in a non-Hermitian lattice," *Phys. Rev. Lett.* **116**, 133903 (2016).
- [24] D. Leykam, K. Y. Bliokh, C. Huang, Y. D. Chong, and F. Nori, "Edge modes, degeneracies, and topological numbers in non-Hermitian systems," *Phys. Rev. Lett.* **118**, 040401 (2017).
- [25] H. Shen, B. Zhen, and L. Fu, "Topological band theory for non-Hermitian hamiltonians," *Phys. Rev. Lett.* **120**, 146402 (2018).
- [26] E. J. Bergholtz, J. C. Budich, and F. K. Kunst, "Exceptional topology of non-Hermitian systems," *Rev. Mod. Phys.* **93**, 015005 (2021).
- [27] A. Guo *et al.*, "Observation of \mathcal{PT} -symmetry breaking in complex optical potentials," *Phys. Rev. Lett.* **103**, 093902 (2009).
- [28] R. El-Ganainy, K. G. Makris, M. Khajavikhan, Z. H. Musslimani, S. Rotter, and D. N. Christodoulides, "Non-Hermitian physics and PT symmetry," *Nat. Phys.* **14**, 11 (2018).
- [29] L. Xiao, T. Deng, K. Wang, Z. Wang, W. Yi, and P. Xue, "Observation of non-bloch parity-time symmetry and exceptional points," *Phys. Rev. Lett.* **126**, 230402 (2021).
- [30] S. Redner, *A Guide to First-Passage Processes* (Cambridge University Press, 2001).
- [31] R. Metzler, G. Oshanin, and S. Redner, *First-Passage Phenomena and Their Applications* (World Scientific, Singapore, 2014).
- [32] Y. Aharonov, J. Oppenheim, S. Popescu, B. Reznik, and W. G. Unruh, "Measurement of time of arrival in quantum mechanics," *Phys. Rev. A* **57**, 4130 (1998).
- [33] H. Friedman, D. A. Kessler, and E. Barkai, "Quantum walks: The first detected passage time problem," *Phys. Rev. E* **95**, 032141 (2017).
- [34] Q. Liu, K. Ziegler, D. A. Kessler, and E. Barkai, "Driving quantum systems with repeated conditional measurements," (2021), [arXiv:2104.06232](https://arxiv.org/abs/2104.06232).
- [35] V. Dubey, C. Bernardin, and A. Dhar, "Quantum dynamics under continuous projective measurements: Non-

- Hermitian description and the continuum-space limit,” *Phys. Rev. A* **103**, 032221 (2021).
- [36] F. Thiel, I. Mualem, D. Meidan, E. Barkai, and D. A. Kessler, “Dark states of quantum search cause imperfect detection,” *Phys. Rev. Research* **2**, 043107 (2020).
- [37] Here the right eigenvector is $U(\tau)^{-1} |\psi_d\rangle$ with $\xi = 0$, namely lowest eigenvalue of \mathcal{S} in the absolute value sense.
- [38] More generally $\tau = 2\pi/N\gamma + 2j\pi/\gamma$ and j is a non-negative integer.
- [39] S. Mittal, J. Fan, S. Faez, A. Migdall, J. M. Taylor, and M. Hafezi, “Topologically robust transport of photons in a synthetic gauge field,” *Phys. Rev. Lett.* **113**, 087403 (2014).
- [40] R. Keil, C. Poli, M. Heinrich, J. Arkininstall, G. Weihs, H. Schomerus, and A. Szameit, “Universal sign control of coupling in tight-binding lattices,” *Phys. Rev. Lett.* **116**, 213901 (2016).
- [41] O. Boada, L. Novo, F. Sciarrino, and Y. Omar, “Quantum walks in synthetic gauge fields with three-dimensional integrated photonics,” *Phys. Rev. A* **95**, 013830 (2017).
- [42] S. Mittal, V. V. Orre, G. Zhu, M. A. Gorkach, A. Poddubny, and M. Hafezi, “Photonic quadrupole topological phases,” *Nat. Photonics* **13**, 692 (2019).
- [43] Y. Chen, X. Chen, X. Ren, M. Gong, and G. C. Guo, “Tight-binding model in optical waveguides: Design principle and transferability for simulation of complex photonics networks,” *Phys. Rev. A* **104**, 023501 (2021).
- [44] T. Manovitz, Y. Shapira, N. Akerman, A. Stern, and R. Ozeri, “Quantum simulations with complex geometries and synthetic gauge fields in a trapped ion chain,” *PRX Quantum* **1**, 020303 (2020).
- [45] C. Monroe *et al.*, “Programmable quantum simulations of spin systems with trapped ions,” *Rev. Mod. Phys.* **93**, 025001 (2021).
- [46] J. Majer *et al.*, “Coupling superconducting qubits via a cavity bus,” *Nature* **449**, 443 (2007).
- [47] A. Dewes, R. Lauro, F. R. Ong, V. Schmitt, P. Milman, P. Bertet, D. Vion, and D. Esteve, “Quantum speeding-up of computation demonstrated in a superconducting two-qubit processor,” *Phys. Rev. B* **85**, 140503(R) (2012).
- [48] X. Gu, A. F. Kockum, A. Miranowicz, Y. Liu, and F. Nori, “Microwave photonics with superconducting quantum circuits,” *Phys. Rep.* **718**, 1 (2017).
- [49] A. Periwal, E. S. Cooper, P. Kunkel, F. W. Julian, J. D. Emily, and S. S. Monika, “Programmable interactions and emergent geometry in an array of atom clouds,” *Nature* **600**, 630 (2021).
- [50] K. Fang, Z. Yu, and S. Fan, “Photonic Aharonov-Bohm effect based on dynamic modulation,” *Phys. Rev. Lett.* **108**, 153901 (2012).
- [51] S. Mukherjee, M. Di Liberto, P. Öhberg, R. R. Thomson, and N. Goldman, “Experimental observation of Aharonov-Bohm cages in photonic lattices,” *Phys. Rev. Lett.* **121**, 075502 (2018).

Supplemental Material for “Special purpose quantum graphs for guaranteed and fast search times”

Quancheng Liu, David A. Kessler, and Eli Barkai

*Department of Physics, Institute of Nanotechnology and Advanced Materials, Bar-Ilan University, Ramat-Gan
52900, Israel*

MATRIX DETERMINANT LEMMA

We provide details on the derivation of Eq. (2) using the matrix determinant lemma [1]. Suppose A is an invertible square matrix and u, v are column vectors, then the matrix determinant lemma states:

$$\det|A + uv^T| = (1 + v^T A^{-1}u)\det|A|, \quad (\text{S1})$$

where uv^T is the outer product of the vectors u and v . We are interested in the eigenvalues of the survival operator $\det|\xi - \mathcal{S}(\tau)| = 0$ with $\mathcal{S}(\tau) = (1 - |\psi_d\rangle\langle\psi_d|)U(\tau)$ as defined in the main text. Substituting \mathcal{S} into the matrix determinant, we have

$$\det|\xi - \mathcal{S}(\tau)| = \det|\xi - U(\tau) + |\psi_d\rangle\langle\psi_d|U(\tau)|. \quad (\text{S2})$$

As discussed in the main text, to prevent the appearance of dark states, which are not optimal for the quantum search, we have conditioned $\det|\xi - U(\tau)| \neq 0$. Hence $\xi - U(\tau)$ is an invertible square matrix. If we denote $\xi - U(\tau)$ as the matrix A , it fits the condition for the matrix determinant lemma. We then let $u = |\psi_d\rangle$, and $v^T = \langle\psi_d|U(\tau)$. Using Eq. (S1), we have:

$$\det|\xi - \mathcal{S}(\tau)| = \xi \det|\xi - U(\tau)| \langle\psi_d| \frac{1}{\xi - U(\tau)} |\psi_d\rangle. \quad (\text{S3})$$

This is the formula we utilize in the main text. Now the determinant of $\xi - \mathcal{S}(\tau)$ is divided into three parts, and we discuss them separately in the main text.

FIGURE PREPARATION

Numerical Simulation Methods

To prepare the plots, we simulate the search process directly based on Eq. (1). We first construct the search Hamiltonians for the crawl graph and funnel graph using Eqs. (11) and (S12). In the simulation, we set $N = 50$ (for preparation of Fig. 2). The initial state of the system is usually a node of the graph namely $|\psi_{\text{in}}\rangle = |x\rangle$. We represent it by a vector of dimension N . For example, if the system is initially localized on node 0, we set the first entry of the vector to be one and all the rest remains zero. With the initial state and funnel/crawl Hamiltonians, we numerically calculate ϕ_1 , which is the overlap between the wave function at time τ and the search target $|\psi_d\rangle$, namely $\phi_1 = \langle\psi_d|U(\tau)|\psi_{\text{in}}\rangle$. The square of $|\phi_1|$ is the probability that we detect the particle in the first measurement at time $t = \tau$, which is recorded for plotting Fig. 2. We then turn to the calculation of F_2 . In the first step, the failed measurement (at time τ) projects out the state on $|\psi_d\rangle$. This is done by setting the state that overlap with $|\psi_d\rangle$ to zero, in other words, we mimic the back-action of projection $(1 - |\psi_d\rangle\langle\psi_d|)$. For example, let $|\psi_d\rangle = |0\rangle$, then after the measurement, the state of the system on node 0 is zero. The measured state is the new initial state for the calculation of F_2 . Similar to the calculation of F_1 , we let the system evolve for time τ by $U(\tau)$, then calculate the overlap between the state of the system and search target, which is ϕ_2 . The search probability $F_2 = |\phi_2|^2$. Such procedure is repeated, we numerically calculate F_3, F_4, \dots, F_n . The results are plotted in Fig. 2 for the crawl (a) and funnel (b) models.

Figure Details

We now provide further details of the figures.

- Fig. 1(a). Schematic plot of the crawl graph Hamiltonian Eq. (11) of size 20×20 . Here we set $\gamma = 1$ and subsequently. In Eq. (11), we have a typical matrix element $1/[1 - \exp(i\theta)]$, which can be formally written as $1/[1 - \exp(i\theta)] = R \exp(i\Phi)$. The R represents the coupling strength between the nodes, in the figure we utilize the thickness of the connecting line to represent its magnitude. The R decrease as the distance between the nodes becomes longer. For example, $R_{0,1} = R_{0,19} > R_{0,2} = R_{0,18} > R_{0,3} = R_{0,17} > \dots > R_{0,10}$. The colors represent the phases Φ , where the phases $\pi > \Phi > \pi/2$. The on site energy of the nodes are equal to zero, hence all of them are plotted gray. Geometrically, the system is rotationally invariant.
- Fig. 1(b). Schematic plot of the funnel Hamiltonian Eq. (S12) of size 20×20 . The matrix elements in Eq. (S12) are real, and again we utilize the thickness of the line connecting the nodes to represent the hopping rate magnitude. Now the on-site energies are not identical, and we present this variation by the colors. The detection node is specialized for this model, and we mark this node in the graph. The on-site energies increase linearly for the nodes from 1 to $N - 1$, and for the search node, the on-site energy is approximately $N/2$.
- Fig. 2(a). Search probability F_n versus measurement steps n for the crawl graph. Here the graph has 50 nodes. We choose the initial states to be the nodes of the graph, namely $|\psi_{\text{in}}\rangle = |0\rangle, |1\rangle, \dots, |49\rangle$. As we discussed in the main text, the search state can be any node of the graph, but here for demonstration, we choose $|\psi_{\text{d}}\rangle = |0\rangle$. We numerically simulate the search process with the method we discussed above. As shown in the figure, the search is deterministic, namely, we detect the walker with probability one at some specified times, as described in the text.
- Fig. 2(b). Search probability F_n versus measurement steps n for the funnel model. Here we set $N = 50$ and the search target is $|\psi_{\text{d}}\rangle = |0\rangle$. Again, we choose the initial state to be a node of the graph and x goes from 0 to 49. We then apply the simulation approach discussed above, which gives the statistics of F_n as shown in the figure. For any initial state, the detection of the state is guaranteed with probability one within N measurements. There is a clear cutoff for F_n when $n > N$, which drops to zero, namely $F_{n > N} = 0$. The upper bound of the search time is found when $|\psi_{\text{in}}\rangle = |0\rangle = |\psi_{\text{d}}\rangle$, where $F_{50} = 1$ and $F_{n \neq 50} = 0$, and in this case the detection time is 2π .
- Fig. 3 describes the unitary evolution without measurements (non-monitored quantum walks) for the crawl Hamiltonian (a) and funnel model (b). We plot the probability of finding the walker on node x , $|\langle \psi(t) | x \rangle|^2$ versus x , and for continuous-time t (in the unit $\tau/10$). Here, for both graphs, we choose $N = 20$ and the initial state is $|0\rangle$. We record $|\langle \psi(t) | x \rangle|^2$ for all the nodes with sampling time interval $\tau/10$. As shown in the figure, the wave function of the crawl graph is localized at specific nodes of the graph at times $\tau, 2\tau, 3\tau, \dots$. In the funnel mode (b), starting for a localized state $|0\rangle$, the wave function first spreads to the whole graph. Then it returns to the localized state $|0\rangle$. The system is recurrent, which is rooted in the periodicity of the energy spectrum we design.

DETAILS ON THE DERIVATION OF EQ. 6

We present the derivation of Eq. (6). As discussed in the main text, the eigen function of the survival operator $\mathcal{S}(\tau)$ can be written as $\xi \sum_{k=0}^{N-1} p_k / [\xi - \exp(-iE_k\tau)] = 0$. Here, we denote the summation as I . With Eq. (5), we have

$$I = \frac{\xi}{N} \sum_{k=0}^{N-1} \frac{1}{\xi - \exp(-i2\pi k/N)} = -\frac{\xi}{N} \sum_{k=0}^{N-1} \frac{\exp(i2\pi k/N)}{1 - \xi \exp(i2\pi k/N)}, \quad (\text{S4})$$

where we multiply both numerator and denominator by $\exp(-i2\pi k/N)$ for each terms in the summation. We first Taylor expand $1/[1 - \xi \exp(i2\pi k/N)]$ and get

$$I = -\frac{\xi}{N} \sum_{k=0}^{N-1} \exp(i2\pi k/N) \sum_{j=0}^{\infty} [\xi \exp(i2\pi k/N)]^j = -\frac{\xi}{N} \sum_{k=0}^{N-1} \sum_{j=0}^{\infty} \xi^j \exp[i2\pi k(j+1)/N]. \quad (\text{S5})$$

We then calculate I by changing the order of the summations. Namely we first perform the summation over k , which is a geometric progression with common ratio $\exp[i2\pi(j+1)/N]$. By calculating the geometric progression, we have:

$$I = -\frac{\xi}{N} \sum_{j=0}^{\infty} \xi^j \sum_{k=0}^{N-1} \exp[i2\pi k(j+1)/N] = \frac{\xi}{N} \sum_{j=0}^{\infty} \xi^j \frac{1 - \exp(i2\pi j)}{1 - \exp[i2\pi(j+1)/N]}. \quad (\text{S6})$$

Since j is an integer, the numerator $1 - \exp(i2\pi j)$ always equals to zero. The whole fraction is non-zero only when the denominator $1 - \exp[i2\pi(j+1)/N]$ also equals to zero. That is possible and happens when $\exp[i2\pi(j+1)/N] = 1$, namely $j = nN - 1$, where n is an integer and goes from 1 to infinity (if n starts from 0, $j = -1$, which goes beyond the regime of j). When both numerator and denominator equal to zero, using L'Hospital's rule, we have

$$\lim_{j \rightarrow nN-1} \frac{1 - \exp(i2\pi j)}{1 - \exp[i2\pi(j+1)/N]} = N, \quad n = 1, 2, 3, \dots \quad (\text{S7})$$

Hence in Eq. (S6), we only need to sum the terms when $j = nN - 1$, and the other terms are simply zero. We replace the summation index j with n , where n goes from 1 to infinity. Then for the summation I , we have:

$$I = \frac{\xi}{N} \sum_{j=nN-1} \xi^j N = \frac{\xi}{N} \sum_{n=1}^{\infty} \xi^{nN-1} N = \sum_{n=1}^{\infty} \xi^{nN} = -\frac{\xi^N}{1 - \xi^N}. \quad (\text{S8})$$

These are the details of the derivation of Eq. (6) in the main text.

PROOF OF THE ORTHOGONAL OF STATES $|Q_k\rangle$

We present the proof that the states $|Q_0\rangle, |Q_1\rangle, |Q_2\rangle, \dots, |Q_{N-1}\rangle$ are orthogonal with each other, namely $\langle Q_l|Q_m\rangle = \delta_{lm}$. The state $|Q_k\rangle$ is defined by the unitary evolution operator U_s to the power k times the search target $|\psi_d\rangle$, where $U_s = \exp(-iH_s\tau)$ and H_s are search Hamiltonian satisfying Eq. (5). To show the orthogonality, we first expanded $|\psi_d\rangle$ in the energy basis, which leads to:

$$|Q_m\rangle = (U_s)^m |\psi_d\rangle = \sum_{k=0}^{N-1} (U_s)^m \langle E_k|\psi_d\rangle |E_k\rangle = \sum_{k=0}^{N-1} \exp(-imE_k\tau) \langle E_k|\psi_d\rangle |E_k\rangle = \sum_{k=0}^{N-1} \exp(-i2\pi km/N) \langle E_k|\psi_d\rangle |E_k\rangle. \quad (\text{S9})$$

Here we have used the fact $E_k\tau = 2\pi k/N$. Similarly, we can find the representation of the state $|Q_l\rangle$ in the energy basis. We then calculate the overlap between the states $|Q_m\rangle$ and $|Q_l\rangle$. We have

$$\langle Q_l|Q_m\rangle = \sum_{k=0}^{N-1} \sum_{k'=0}^{N-1} \langle E_k|\psi_d\rangle \langle E_{k'}|\psi_d\rangle \exp[i2\pi(kl - k'm)/N] \langle E_k|E_{k'}\rangle = \sum_{k=0}^{N-1} |\langle \psi_d|E_k\rangle|^2 \exp[i2\pi k(l - m)/N]. \quad (\text{S10})$$

The square of the overlap between the detected state $|\psi_d\rangle$ and the energy state $|E_k\rangle$ is denoted as p_k in the main text, namely $p_k = |\langle \psi_d|E_k\rangle|^2$. Eq. (5) states this value is a dependent of k for the search Hamiltonian H_s , where $p_k = 1/N$. So for Eq. (S10), we only need to calculate the summation of $\exp[i2\pi k(l - m)/N]$ from $k = 0$ to $N - 1$. This has been done also in Eq. (S6), where $(j + 1)$ in Eq. (S6) is replaced by $(l - m)$ here. We then have:

$$\langle Q_l|Q_m\rangle = \frac{1}{N} \sum_{k=0}^{N-1} \exp[i2\pi k(l - m)/N] = \frac{1}{N} \frac{\exp[i2\pi(l - m)] - 1}{\exp[i2\pi(l - m)/N] - 1}. \quad (\text{S11})$$

Using Eq. (S7), $\langle Q_l|Q_m\rangle$ is non-zero only when $l - m = 0, N, 2N, \dots$. Here $N - 1 \geq l \geq 0$ and $N - 1 \geq m \geq 0$. Hence only when $l = m$ we have $\langle Q_l|Q_m\rangle = 1$, otherwise $\langle Q_l|Q_m\rangle = 0$. Namely $\langle Q_l|Q_m\rangle = \delta_{lm}$. This is the conclusion we used in the main text. Another thing to notice is that, since the $|Q_k\rangle$ are generated by the unitary operators, it is naturally normalized. Hence the states $\{|Q_0\rangle, |Q_1\rangle, |Q_2\rangle, \dots, |Q_{N-1}\rangle\}$ forms a complete and normalized space.

FUNNEL MODEL HAMILTONIAN

We provide details on the funnel Hamiltonian and its explicate presentation. In this model, the search target $|\psi_d\rangle = |0\rangle$. As before, the spatial nodes of the graph are denoted $|x_i\rangle$, and $i = 0, 1, \dots, N - 1$. We start with the energy state $|E_0\rangle = \left\{1/\sqrt{N}, -\sqrt{(N-1)/N}, 0, 0, \dots\right\}$, where $1/\sqrt{N}$ fulfills the first condition in Eq. (5) and $-\sqrt{(N-1)/N}$ stands for normalization. We then construct the energy state $|E_1\rangle$. It should be orthogonal with $|E_0\rangle$ and in agreement with the condition in Eq. (5). We find $|E_1\rangle = \left\{1/\sqrt{N}, 1/\sqrt{N(N-1)}, -\sqrt{(N-2)/(N-1)}, 0, 0, \dots\right\}$. Again, the first term in $|E_1\rangle$ leads to $|\langle E_1|0\rangle|^2 = 1/N$. The

second entry guarantees $\langle E_0|E_1\rangle = 0$, and the third entry is for normalization. Following the construction procedure, we have $|E_2\rangle = \left\{1/\sqrt{N}, 1/\sqrt{N(N-1)}, 1/\sqrt{(N-2)(N-1)}, -\sqrt{(N-3)/(N-2)}, 0, 0, \dots\right\}$, and in general $|E_{i \neq N-1}\rangle = \left\{1/\sqrt{N}, 1/\sqrt{N(N-1)}, \dots, 1/\sqrt{(N+2-k)(N+1-k)}, \dots, -\sqrt{(N-1-i)/(N-i)}, 0, 0, \dots\right\}$, where k is the index for the k -th entry and $2 \leq k \leq i$. This general representation $|E_i\rangle$ can help us construct the states $|E_0\rangle, |E_1\rangle, \dots, |E_{N-2}\rangle$, but not $|E_{N-1}\rangle$. Let us explain this and then show how to construct $|E_{N-1}\rangle$. When $i = N-2$, we have $|E_{N-2}\rangle = \left\{1/\sqrt{N}, 1/\sqrt{N(N-1)}, \dots, 1/\sqrt{6}, -1/\sqrt{2}\right\}$. Now we cannot utilize the procedure we did before to construct $|E_{N-1}\rangle$, since roughly speaking there is no additional space for the normalization. So how to construct the last energy state? We notice the last term in $|E_{N-2}\rangle$ is $-1/\sqrt{2}$, which is special. Let us consider a state where the first $N-1$ terms are the same as those in $|E_{N-2}\rangle$, and the only different one is the last term, where we change the $-1/\sqrt{2}$ to $1/\sqrt{2}$. We can see such a state is orthogonal with $|E_{N-2}\rangle$ and also normalized. This is the last energy state, i.e., $|E_{N-1}\rangle = \left\{1/\sqrt{N}, 1/\sqrt{N(N-1)}, \dots, 1/\sqrt{6}, 1/\sqrt{2}\right\}$. It is also easy to show that this state is orthogonal with respect to the other state, $|E_{N-3}\rangle, |E_{N-4}\rangle, \dots, |E_0\rangle$. We then have N orthogonal and normalized states fulfill the conditions in Eq. (5).

For the equal distance energies, we set $E_0 = 0, E_1 = \gamma, E_2 = 2\gamma, \dots, E_{N-1} = (N-1)\gamma$, the resulting Hamiltonian is

$$H = \frac{\gamma}{2} \begin{bmatrix} N-1 & H_{0,1} & H_{0,2} & \cdots & H_{0,N-1} \\ H_{0,1} & 1 & H_{1,2} & \cdots & H_{1,N-1} \\ H_{0,2} & H_{1,2} & 3 & \cdots & H_{2,N-1} \\ \vdots & \vdots & \vdots & \ddots & \vdots \\ H_{0,N-1} & H_{1,N-1} & H_{2,N-1} & \cdots & 2N-3 \end{bmatrix} \quad (\text{S12})$$

where $H_{0,m} = \sqrt{(N-m)(N-m+1)/(m+1)}$ ($m \neq 0$) and $H_{j,m} = \sqrt{(N-m+1)(N-m)/[(N-j+1)(N-j)]}$ ($j \neq 0, n$). We call this approach the funnel model.

[1] D. A. Harville, *Matrix Algebra From a Statistician's Perspective* (Springer, New York, 1997).